



HHS Public Access

Author manuscript

Nat Commun. Author manuscript; available in PMC 2014 February 24.

Published in final edited form as:

Nat Commun. 2013 ; 4: 2585. doi:10.1038/ncomms3585.

Evidence for distinct human auditory cortex regions for sound location versus identity processing

Jyrki Ahveninen¹, Samantha Huang¹, Aapo Nummenmaa¹, John W. Belliveau^{1,2}, An-Yi Hung¹, Iiro P. Jääskeläinen³, Josef P. Rauschecker⁴, Stephanie Rossi¹, Hannu Tiitinen³, and Tommi Raij¹

¹Harvard Medical School – Athinoula A. Martinos Center for Biomedical Imaging, Department of Radiology, Massachusetts General Hospital, Bldg. 149, 13th St., Charlestown, MA 02129, USA

²Harvard-MIT Division of Health Sciences and Technology, Cambridge, MA, USA

³Department of Biomedical Engineering and Computational Science (BECS), Aalto University School of Science, Espoo, FIN-00076 Aalto, FINLAND

⁴Laboratory of Integrative Neuroscience and Cognition, Department of Neuroscience, Georgetown University Medical Center, New Research Building, Room WP 15, 3900 Reservoir Road, NW Washington, DC 20057-1460, USA

Abstract

Neurophysiological animal models suggest that anterior auditory cortex (AC) areas process sound-identity information, whereas posterior ACs specialize in sound location processing. In humans, inconsistent neuroimaging results and insufficient causal evidence have challenged the existence of such parallel AC organization. Here we transiently inhibit bilateral anterior or posterior AC areas using MRI-guided paired-pulse transcranial magnetic stimulation (TMS) while subjects listen to Reference/Probe sound pairs and perform either sound location or identity discrimination tasks. The targeting of TMS pulses, delivered 55–145 ms after Probes, is confirmed with individual-level cortical electric-field estimates. Our data show that TMS to posterior AC regions delays reaction times (RT) significantly more during sound location than identity discrimination, whereas TMS to anterior AC regions delays RTs significantly more during sound identity than location discrimination. This double dissociation provides direct causal support for parallel processing of sound identity features in anterior AC and sound location in posterior AC.

Users may view, print, copy, download and text and data- mine the content in such documents, for the purposes of academic research, subject always to the full Conditions of use: http://www.nature.com/authors/editorial_policies/license.html#terms

Corresponding Author: Jyrki Ahveninen, Ph.D., MGH/MIT/HMS-Martinos Center, Bldg. 149 13th Street, Charlestown MA 02129, Phone (617) 726-6584; fax (617) 726-7422, jyrki@nmr.mgh.harvard.edu.

The authors declare no competing financial interests.

Author Contributions

J.A., I.P.J., J.P.R., and T.R. designed the study; J.A., S.H., A.Y.H., S.R., and T.R. performed the experiments; A.N., J.W.B., and T.R. contributed new analysis tools; J.A., S.H., A.Y.H., S.R., and T.R. analyzed data; J.A., S.H., A.N., J.W.B., A.Y.H., I.P.J., J.P.R., S.R., H.T., and T.R. wrote the manuscript.

The content is solely the responsibility of the authors and does not necessarily represent the official views of the funding agencies.

Introduction

A number of studies support the theory that sound identity information is processed in anterior and spatial features in posterior aspects of non-primary auditory cortices (AC) ¹⁻⁴, which project to distinct inferior frontal “what” and posterior parietal/superior prefrontal “where” areas ⁵⁻¹⁰, respectively. In humans, posterior AC regions, encompassing the planum temporale (PT) and posterior superior temporal gyrus (STG), are activated by a range of audiospatial cues ^{3, 11-14}, while AC areas anterolateral to Heschl’s gyrus (HG), extending to the anterior STG and the planum polare (PP), are sensitive to a various sound identity features ^{3, 10, 15-20}. Yet, several neuroimaging studies suggest that the posterior non-primary ACs also respond to non-spatial sounds, such as “spectral motion” ²¹ and/or phonetic features ^{22, 23}, which has led to an alternative interpretation that the model of separate sound identification *vs.* localization regions in human ACs is inaccurate (see, *e.g.*, ^{22, 24, 25}). However, when interpreting the existing evidence in humans, it is noteworthy that previous studies have almost exclusively used observational neuroimaging techniques that reveal correlations, but cannot prove causality, *i.e.*, that these AC areas are required for sound identification *vs.* localization.

A powerful way to causally corroborate neuroimaging-based models is to turn the participating brain areas off one by one and observe how brain functions and behaviors change. Classically, cognitive neuropsychologists have applied this kind of approach in humans, by seeking double dissociations in functional deficits between subjects with different kinds of lesions. Pioneering studies in patients with lesions extending to different aspects of the temporal cortex have provided support for the AC dual pathway model in humans ^{6, 26, 27}. However, the specificity of this approach is limited because it is rare to find patients with lesions focused to certain part of the human AC only. For example, in one previous human lesion study on the dual pathway model ²⁷, the damage extended to extra-auditory frontoparietal regions, as well as to subcortical gray and white matter in almost all studied patients. Lesion studies are, further, complicated by potential differences in pre-morbid abilities between subjects, and compensatory changes in other brain areas related to the long-term effects of the lesion. A more accurate approach, available in animal models, is reversible inactivation of individual brain regions by cooling. A recent dual-pathway study ⁴ showed that local cooling of posterior *vs.* anterior auditory fields of cat AC causes selective deficits in sound localization *vs.* identity discrimination tasks, respectively. However, analogous confirmation in humans is still lacking. Further, although the aforementioned cooling study provided strong longitudinal evidence for the lack of long-term changes in the manipulated cat AC areas ⁴, other studies using the cooling technique ²⁸⁻³⁰, or alternative means of local deactivation ³¹ or deafferentation ^{32, 33}, imply that a complete deactivation of any cortical region will, within minutes ³⁰, result in profound changes in other areas that are connected to the manipulated region. For example, pharmacological temporary deactivation of AC leads to profound changes at the preceding subcortical stages of sound processing ³⁴. This raises the question if the observed behavioral changes reflect the properties of the cooled area alone or also that of other areas. Unfortunately, there are no prior studies in any species that have investigated processing of sound identity *vs.* location information using

very transient disruption of functionality (e.g., brief cortical electrical stimulation) that is less likely to induce wider spread network changes or reorganization.

Instantaneous (<50 ms) and local modulations of human brain activity can be non-invasively induced using transcranial magnetic stimulation (TMS). The paired-pulse TMS (ppTMS) technique is especially powerful in this regard, as applying two TMS pulses at about 1–4 ms apart with a specific intensity ratio causes short-interval intracortical inhibition (SICI), effectively creating a relatively focal “functional lesion” lasting only tens of milliseconds^{35, 36}. Paired-pulse TMS therefore allows one to create short-lived functional deactivations in the human brain with high spatial and temporal accuracy, and in the context of specific behavioral paradigms, to determine the functional role of the targeted areas. This technique can be applied to healthy subjects, and the short duration of the effects allows subjects to serve as their own controls, and any compensatory functional re-organization is unlikely to occur. SICI effects emerge only when a brain area receives two TMS pulses at a specific intensity ratio, which limits them to occur locally at the TMS target area³⁷. In comparison to repetitive TMS (rTMS), in which the target area receives trains of pulses for a longer period of time, or cooling deactivations used in animal models, ppTMS probably results in less pronounced effects in remote areas connected to the TMS target. Furthermore, recent advances in MRI-guided on-line navigation systems and focal stimulation coils allow reasonably accurate targeting, influencing spatially much smaller regions than most naturally occurring lesions.

To our knowledge, there are no prior studies applying TMS to different sub-regions of the supratemporal AC. However, we stipulated that such an approach might be fruitful, given that TMS to sound processing areas outside the superior temporal AC has separately modulated processing of auditory object identity and spatial localization. Specifically, a recent study³⁸ suggested that TMS of the left inferior frontal gyrus (IFG) that is associated with the auditory “what” stream¹ impairs identification of sound patterns associated with words, whereas TMS of occipital and posterior parietal cortex areas, partially overlapping with the putative auditory posterior-dorsal “where” auditory stream¹, modulates sound localization performance^{39, 40}. Recently, it was also shown that rTMS to inferior parietal lobule produces selective impairments in auditory motion processing⁴¹.

Here, we utilize MRI-guided ppTMS to validate the model^{1–4} postulating separate areas for spatial vs. sound identity processing in human AC. Our results demonstrate a double dissociation that supports this parallel processing model, with ppTMS to anterior AC delaying reaction times (RT) most prominently during sound identity discrimination and ppTMS to posterior AC delaying RTs most prominently during sound location discrimination. Cortical electric-field (E-field) estimates confirm that TMS pulses reached the intended targets in all subjects.

Results

TMS effects on sound location and identity discrimination

Ten normal-hearing participants were presented with Reference/Probe sound pairs (Figure 1). In the Spatial task, subjects discriminated whether Probe arrived from 5° to the left or 5°

to the right relative to Reference (25° to the right). In the Identity task, subjects discriminated whether the amplitude-modulation (AM) frequency of Probe was 1/6 octaves lower (35.6 Hz) or higher (44.9 Hz) than that of Reference (40 Hz). The experiment was divided into eight runs, each containing 80 trials. Fifty percent of the trials did not include TMS and therefore provided baseline reaction time (RT) data. For the other 50% of trials, bilateral TMS was delivered 55–145 ms after the Probes, at either the anterior or the posterior non-primary ACs.

RT delays caused by TMS were analyzed using a contemporary “real-time” linear mixed modeling approach^{42, 43} (for details, see Methods) that is becoming increasingly popular amongst behavioral and cognitive scientists. This linear mixed approach models individual task responses in each task condition/subject, and brings longitudinal temporal dependencies into the statistical model, thus allowing for better control for a number of biases that have been difficult to model in more traditional analyses where task responses are first aggregated within subjects^{42, 43}. For RT lags, we found task-specific modulations for the anterior *vs.* posterior non-primary AC TMS. According to Markov chain Monte Carlo (MCMC) simulations, there was a highly significant interaction between the task type and the TMS target location ($t=3.3$, $P_{\text{MCMC}}=0.001$; $N_{\text{Subjects}}=10$, $N_{\text{Trials/Subject}}=640$; note that conventional t/F -distributions and degrees of freedom are not directly applicable to linear mixed models). Figure 2 shows the estimated marginal means of RT lags caused by TMS in each task condition and at each target location, as derived from the linear mixed model. These data show that the RT lags were more pronounced (a) after posterior than anterior AC TMS during the Spatial Task ($P<0.05$, Tukey adjusted; $N_{\text{Subjects}}=10$, $N_{\text{Trials/Subject}}=640$) and (b) after anterior than posterior AC TMS during the Identity task ($P<0.05$, Tukey adjusted; $N_{\text{Subjects}}=10$, $N_{\text{Trials/Subject}}=640$). There was also a slightly weaker but significant main effect of TMS target location ($t=2.2$, $P_{\text{MCMC}}<0.05$; $N_{\text{Subjects}}=10$, $N_{\text{Trials/Subject}}=640$). The main effect of task was non-significant, showing that there were no significant difficulty differences between the Spatial and Identity tasks. Group averages of RTs in different task conditions, separately for different TMS latencies, are shown in Table 1. An additional analysis did not find any significant interactions between the task, target location, and TMS pulse latency.

For hit rates (HR), the linear mixed model did not indicate significant interaction effects between the task, target location, and TMS treatment. TMS resulted in an overall decrease of 9% in HR (estimated marginal means \pm standard errors: 77 \pm 4% after TMS, 86 \pm 4% with no TMS; $t_{63}=4.1$, $p<0.001$; $N_{\text{Subjects}}=10$, $N_{\text{Trials/Subject}}=640$). The group estimates of HR values in the individual task conditions are shown in Table 2. Finally, Figure 3 shows the variability of task performance, quantified as the standard deviation of RT, in each individual subject during the baseline trials, TMS trials, and across all trials.

Verifying TMS targeting by cortical E-field estimates

The results of electromagnetic modeling analyses, which were conducted to verify the foci of E-fields induced by TMS in each subject, are shown in Figure 4. These data show that the intended targets were successfully stimulated during both posterior and anterior AC TMS conditions. The anterior AC stimulation reached maximal levels at areas anterolateral to

Heschl's gyrus (HG), including anterior STG. The supratemporal areas stimulated during TMS of posterior AC included posterior STG and PT. Further, the E-field distributions were quite focal, resulting in that collateral fields (surrounding the intended target areas), which are largely unavoidable with TMS, did not extend to areas that have been associated with frontal or parietal auditory “what” or “where” pathways. For example, during the anterior TMS pulses, the supra-Sylvian fields reaching the threshold were centered at the central sulcus, far from IFG areas presumed to be associated with the auditory “what” stream beyond AC. During posteriorly targeted TMS, the supra-Sylvian fields were strongest in inferior aspects of parietal cortex. The mean±SD distance along the supratemporal surface of peak E-field values between the anterior vs. posterior stimulation sites was 34±10 mm ($N_{\text{Subjects}} = 10$, $N_{\text{Pulse pairs/Location}} = 160$) in the left and 37±10 mm in the right hemisphere ($N_{\text{Subjects}} = 10$, $N_{\text{Pulse pairs/Location}} = 160$).

Continuous tracking of the coils and head position with the navigation device indicated that movement was minimal during the experiment (group level mean of individually computed SDs for coil/head movements was 1.2 mm). This excludes the possibility that the differences between runs would have been caused by head/coil movements leading to stimulation of different brain areas.

Discussion

Here, we studied the effects of transient focal AC deactivations induced by TMS⁴⁴ on processing of object-identity vs. spatial aspects of auditory stimuli. TMS pulse pairs targeted at anterior non-primary AC areas produced more pronounced RT lags during sound identity than location discrimination performance. In contrast, TMS targeted at posterior non-primary AC areas delayed RTs significantly more during the audiospatial than identity task. The linear mixed modeling analyses showed a corresponding significant interaction between the auditory task and anatomical target location on TMS-induced RT lags. These results provide direct causal support for distinct human AC regions for sound location and identity processing, which so far has been studied in healthy humans mainly using neuroimaging methods. The study also offers proof-of-principle for using TMS for studies on human AC functional anatomy.

Previous studies have suggested that delivering paired-pulse TMS at the presently-used intra-pair interval of 2.5 ms triggers transient intracortical inhibition that lasts for up to a few tens of milliseconds³⁶. Here, the TMS pulses were delivered at four latencies between 55 and 145 ms after sound onset. This encompasses the time window during which the MEG/EEG response N1 typically ascends, peaks, and descends in the posterior and anterior non-primary ACs (e.g.,^{3, 45, 46}). Notably, stimulus-locked neuronal processes occurring at these latencies at non-primary ACs are also believed to coincide with the emergence of conscious percepts and formation of neuronal representation of sound objects^{45, 46}. One might thus speculate that the present behavioral effects of TMS were caused by increased local inhibition that delayed sound-feature processing in the underlying areas. However, further studies are needed to verify the exact neuronal mechanisms of the presently observed effects.

A large number of investigations in humans (e.g., ^{1-3, 11-14}) and animal models ^{1, 2, 4}, even some of those supporting distributed coding instead of topographical representation of acoustic space ^{47, 48}, are in line with the view that neurons processing spatial features are most abundantly populating the posterior auditory fields. As for the “what” pathway, contradictory findings have been reported, for instance, in recent human neuroimaging studies that have found spread of pitch-related neuroimaging activations also to posterior AC ⁴⁹. This has been interpreted to contradict the existence of a pitch-specific region in the anterolateral AC, previously reported in monkeys ⁵⁰ and humans (e.g., ^{15, 16}). The present study, in which sound identity processing was measured using a task that required discrimination of AM differences (*i.e.*, temporal pitch), however, suggests that anterior AC areas may, indeed, be behaviorally relevant for pitch tasks. Note, however, that the present AM frequencies were slightly closer to the boundary of pitch vs. flutter perception than the typical fundamental frequencies (f_0) used in previous temporal-pitch functional MRI (fMRI) studies; e.g., $f_0=62.5$ Hz in 51 and 83.1 Hz in ¹⁵. Thus, future studies may be needed to see how the present results generalize across different stimulus and task types.

Although previous studies ^{3, 45, 46} have suggested a latency difference of about 10–30 ms between the N1 activation peaks in the posterior “where” vs. anterior “what” regions, the present results regarding TMS latencies were inconclusive. That is, no significant interactions between the task type, TMS target, and TMS latency emerged. Further studies could illuminate whether the interruption of local AC processes have characteristic critical latencies for different task types and subanatomical areas in humans. On the same note, the behavioral effects induced by TMS in the present study were, as fully expected given the more transient nature of neuronal manipulations, more subtle than those produced by recent cooling deactivation studies ⁴ that resulted in complete inactivation of larger extents of AC (and likely also in areas connected to the deactivated regions ^{28, 29}). Instead of a major decrease of HR, we observed RT delays <100 ms. Note also that the current extent of RT lags is logical given the presumed short duration of neuronal effects of ppTMS.

The present study demonstrates the utility of electromagnetic modeling of the TMS induced E-fields at the individual cortical surfaces, and the value of being able to compute surface-based across-subjects averages of the E-fields. To our knowledge this is the first applied TMS study to report such data. Our modeling, specifically, showed that anterior and posterior TMS targeted separate areas in the intended regions, extending from the supratemporal cortex inside the Sylvian fissure to lateral aspects of STG that are more accessible to TMS than the core regions inside the sulcus. It is, however, noteworthy that beyond coil design and selection, TMS does not allow customized shaping of the E-fields, and volume conduction leads to that not only the maximum but also the immediately surrounding areas receive stimulation. For example, despite the fact that our study was based on an MRI-guided on-line navigation system and quite small stimulation coils that allow relatively focal targeting of cortical tissue, not only STG but also the adjacent gyri (albeit with lesser intensities) were stimulated. Yet, our electromagnetic modeling showed that, in the case of anterior AC stimulation, such “collateral” TMS effects in supra-Sylvian regions were clearly more posterior than the inferior frontal “what” stream (including the IFG areas pars opercularis and triangularis), as they actually peaked in the postcentral (*i.e.*, parietal

lobe) regions. Similarly, in the case of the posterior AC target, the supra-Sylvian areas stimulated by ppTMS were restricted to the inferior aspects of parietal lobe, and did not extend into the vicinity of the intraparietal sulcus (IPS) that is a key anatomical locus of the posterior parietal “where” processing stream^{1, 52}. Most importantly, our estimates of TMS-induced E-fields showed clearest and most consistent foci across subjects in the anticipated AC areas.

TMS coil discharges produce both auditory and somatosensory stimulations, which may cause auditory masking effects or non-specific distractions on cognitive performance beyond the neuronal mechanisms of interest. For example, in the present study, ppTMS resulted also in non-specific task modulations (RT increases to ppTMS irrespective of target location) that might have been partially affected by these biases. (Note that, here, we used relatively small figure-of-eight of coils that produce less pronounced clicks than larger coils, as well as earpieces that dampen the click.) In previous studies, researchers have therefore applied several types of control conditions to separate the TMS effects of interest from artifacts. For example, one can apply either “sham TMS” or real TMS to a control brain region that does not, presumably, participate in the activity of interest. A complication for using an independent “non-auditory” control region is, however, that a wide network of areas beyond the supratemporal cortex is, either directly or through polymodal associations, activated during active auditory task performance. Indeed, auditory RTs have been shown to be affected by TMS delivered to a great variety of such “extra-auditory” areas^{38–41}. Therefore, in the present study, we applied a factorial design where each of the AC regions of interest, anterior *vs.* posterior, acted as their own control during the two different auditory task domains. Note also that the relatively high spatial focality and short (2.5-millisecond) duration of ppTMS would suggest that the behavioral effects emerge from local inhibition in the target area where SICI occurs. Although spreading influences to connected areas cannot be completely excluded, if present, they are likely much less prominent than those observed with deactivations lasting several orders of magnitude longer^{30–34} used in animal models⁴. Finally, it is possible that certain extracerebral artifacts, such as scalp muscle stimulation, may result in feedback activities that might potentially cause more pronounced effects on processing of sound identity, particularly in the case of speech sounds³⁸. Here, such biases are probably less likely, as the present identity dimension was artificial, not directly linked to speech features.

In summary, TMS to posterior AC regions delayed RTs significantly more during sound location than identity discrimination, whereas TMS to anterior AC regions delays RTs significantly more during sound identity than location discrimination. This double dissociation provides causal support for the parallel processing model^{1–4} postulating that sound identity features are processed in anterior AC and sound location is encoded in posterior AC in humans. These results also demonstrate the potential usefulness of ppTMS for studying functional anatomy of the auditory cortex in humans, especially when combined with forward modeling of the TMS-induced E-fields on the cortical surface. Further studies are needed to verify the exact neuronal mechanisms that underlie the ppTMS cortical effects.

Methods

Subjects and task design

Ten healthy right-handed subjects (5 females, age 22–51 years) with self-reported normal hearing, screened for TMS and MRI contraindications (metal in the body, implanted medical devices, medications affecting the central nervous system, pregnancy, history of seizures/convulsions/fainting/syncope or significant head trauma)⁵³ participated in the study. Human subjects' approval was obtained and voluntary informed consents approved by the Massachusetts General Hospital Institutional Review Board were signed before the experiment. TMS targeted at AC regions might stimulate temporal muscles, the intensity and discomfort of which varies across individuals. The subjects were informed that they could interrupt the experiment at any time, and their willingness to continue was confirmed repeatedly during the session. In each forced-choice RT trial (Figure 1a), subjects were delivered a pair of binaural 300-ms white-noise bursts (50-dB Sensation Level, 10-ms on/off ramps) at a 1-s onset-to-onset interval (S14 Insert headphones, Sensimetrics, Malden, MA). The first sound of each pair was Reference, and the second was Probe. In the **Identity task**, Probe was amplitude modulated (AM) at either 1/6 octaves lower (35.6 Hz) or higher (44.9 Hz) frequency than Reference (40-Hz AM frequency). After the lower-AM Probe, subjects were to press the leftmost of two buttons using their right-hand index finger, and after the higher-AM Probe, the rightmost of these buttons with the right-hand middle finger. In the **Spatial task** (Figure 1a), References were simulated from 25° and Probes from either 20° or 30° to the right along the azimuth, by convolving the reference sound of the Identity task (40 Hz AM) with generic head-related transfer functions (HRTF)⁵⁴. The subjects were instructed to press the leftmost button with the right-hand index finger to the left Probes, and the rightmost button with the right-hand middle finger to the right Probes. Subjects received feedback in both tasks (“OK” or “Wrong” shown during 0.9–1.9 s after each button press). The subsequent trial started 700 ms after the feedback stimulus ended. The trial duration (average across subjects 5.5 s) was, thus, paced by the subjects' performance. The stimuli were presented and behavioral responses recorded on a PC running Presentation 14.2 (Neurobehavioral Systems, Albany, CA), which sent timing information to the TMS stimulators to synchronize the pulses with auditory stimuli. The difficulty of each task was matched *a priori*. Our statistical model (see below) showed no significant main effects of the task (Identity vs. Spatial) for RTs or hit rates (HR), suggesting that the baseline difficulty levels of each task were consistent.

ppTMS design

TMS experiments were conducted in a dimly lit sound-attenuated low-reverberation chamber. The TMS-coil navigation system was co-registered with each subject's structural MRI (3T Siemens TimTrio, multi-echo MPRAGE pulse sequence, TR=2510 ms; 4 echoes with TEs=1.64, 3.5, 5.36, and 7.22 ms; 176 sagittal slices, 1-mm isotropic voxels, 256×256 matrix; flip angle=7°) with respect to the fiducial landmarks (nasion, two preauricular points) and additional scalp points using a 3-D digitizer (Nexstim NBS, Helsinki, Finland). Two-channel TMS was guided with an infrared navigation system that calculates the location and strength of the induced E-field and displays this on the subject's MRI in real-

time (Nexstim NBS, Helsinki, Finland). Subjects' head movements were minimized by using a headrest and a vacuum pillow.

During auditory stimulation/tasks, paired-pulse TMS (80/120% motor threshold; interpolated from previously reported optimal values^{35–37}) with 2.5-ms inter-pulse interval, biphasic waveform, was delivered simultaneously to both hemispheres with two stimulators (MagPro X100 w/MagOption, MagVenture, Denmark) and two figure-of-eight coils (MagPro C-B60, MagVenture, Falun, Denmark). In separate runs, TMS was targeted either to anterior or posterior non-primary AC areas. TMS coil orientation was perpendicular to the individual local curvature of Sylvian fissure, (*i.e.*, about vertical). Bilateral TMS was chosen because sounds are processed simultaneously in both hemispheres, and because previous studies⁴ suggest more consistent effects after bilateral than unilateral AC deactivations. Bilateral TMS, presumably, also helped avoid lateralized distraction effects during Spatial task. Based on previous studies^{3, 46}, the TMS pulse pairs were applied randomly at four different latencies (55, 85, 115, 145 ms) after the probe-sound onset, covering the typical N1(m) activity in ACs.

The experiment was divided into eight runs, each containing 80 trials and lasting on average 7 min 18 s. In each run, TMS was applied in 50% of trials in random order. Each session, thus, included 320 ppTMS events. On average, ppTMS was delivered about every 10–13 s. To avoid making the experiment excessively long, all conditions in one TMS location were always conducted in a row (coil re-targeting may require extra time when two coils are used). The order of TMS locations and task conditions was counterbalanced across subjects.

Anatomical ppTMS target definition

Each subject's anatomical MRIs were segmented and co-registered to volume-based and surface-based standard brain representations using FreeSurfer 5.1 (<http://surfer.nmr.mgh.harvard.edu>). The TMS target locations were selected based on a sample of previously published maximally-activated fMRI^{10, 11, 13–16} and positron emission tomography⁵¹ voxels during audiospatial or sound-object identity processing. More specifically, the posterior AC targets were defined by averaging the peak-voxel Talairach coordinates of contrasts reflecting sound movement vs. rest¹¹, sound direction changes vs. constant stimulation¹³, sound distance vs. intensity changes¹⁴, and spatially shifting vs. stationary sounds¹⁰. When needed, MNI coordinates were converted to Talairach coordinates. The anterior AC targets were defined similarly, based on peak voxels in contrasts reflecting varying vs. fixed pitch^{10, 15, 16}, fixed pitch vs. noise¹⁵, fixed Huggins pitch vs. noise¹⁶, fixed binaural band pitch vs. noise¹⁶, and pitch-strength-by-melody interactions⁵¹. For both targets, average loci were calculated first within, then across studies. The resulting Talairach coordinates [mm] of initial targets were $\{x,y,z\}=\{-52,-30,12\}$ for the left posterior, $\{x,y,z\}=\{-54,0,-5\}$ for the left anterior, $\{x,y,z\}=\{60,-30,11\}$ for the right posterior, and $\{x,y,z\}=\{55,-4,-6\}$ for the right anterior AC (Fig. 1b). These locations were then transformed to each individual subject's brain representations. Finally, before the TMS experiment, an optimized entry point closer to the inner skull was selected, as guided by the E-field estimates produced by the navigation system, to allow the TMS effects to be maximally focused to the target area.

TMS target *post hoc* confirmation

Electromagnetic modeling analyses utilizing realistic anatomy were conducted to estimate the actual cortically induced E-field distributions in each subject. The inner skull surface obtained from Freesurfer MRI reconstructions was used to create a single-layer boundary element model (BEM). The intracranial space was considered as a homogenous isotropic volume conductor. The position and orientation of the TMS coil was exported from the navigator computer in the MRI coordinates and a model for the wire winding geometry was constructed according to manufacturer specifications (MagPro C-B60, MagVenture, Falun, Denmark). TMS-induced E-field amplitudes were computed at the white matter surfaces (extracted using Freesurfer) according to well-established physical principles, as described by Nummenmaa and colleagues⁵⁵. The custom implementation of the numerical methods was done in Matlab (R2012a, The Mathworks, Inc., Natick, MA) utilizing the core routines from the BEM toolbox of⁵⁶. For comparisons across subjects, the cortical activation estimates were co-registered via spherical morphing to a surface-based standard-brain representation⁵⁷, thresholded at 80% of the individual's maximum, and normalized across individuals.

Data analysis

A full factorial design was utilized to control for potential biases caused by the TMS side effects (acoustic clicks, muscle stimulation). Behavioral data, including RTs (correct responses only) and HRs, were recorded separately for each task condition. At the initial screening, trial responses faster or slower than two standard deviations (SD) of each subject's average RT were excluded as outliers (physiologically unreasonable responses, *i.e.*, $RT < 50$ ms or > 4 s, were excluded before this). Statistical analyses were conducted using the R packages lme4, languageR, and lsmeans^{58–60}. Instead of averaging RTs first within subjects, we utilized a linear mixed approach^{42, 43} that models individual responses in each task condition/subject and brings the potential longitudinal biases between successive trials into the statistical model specification. To further mitigate within-session fluctuations (*e.g.* related to the blocked TMS design), we specifically examined the time series of TMS-induced RT lags, obtained by subtracting the within-condition average RT_{Baseline} from each individual RT_{TMS} event. The RT lag time series were, finally, entered into a linear mixed model: The random effects included the subject and trial type (sound direction nested within Spatial task; AM frequency nested within Identity task); The fixed effects included the task (Identity *vs.* Spatial), TMS target location (anterior *vs.* posterior), task-by-TMS-target-location interaction, TMS pulse-pair latency (55–145 ms), age, gender, and the trial-specific sequential predictors (task-block number, trial numbers, RT to preceding baseline trial) controlling for temporal dependencies/autocorrelations. We controlled for potential biases caused by non-normality and homogeneity by examining the model residuals against fitted values. Multicollinearity was addressed by residualizing predictors correlating with each other. The model was weighted by the inverse variances of each subject's behavioral performance.

Our main hypothesis regarded the interaction between the task and TMS target location: We hypothesized that RT lags are significantly larger with TMS targeted to the anterior *vs.* posterior AC during the Identity task, and *vice versa* during the Spatial task. Statistical

significances were presented as Markov chain Monte Carlo (MCMC) estimated *p*-values. *A priori* comparisons were computed based on the main models using the R *lsmeans* package⁶⁰. Finally, HR results were analyzed with a linear mixed model with the task, target location, treatment (TMS vs. no TMS), age, and gender as fixed-effect factors and the subject as a random-effect factor.

Acknowledgments

We thank Mary O’Hara, Nancy Shearer, Chinmayi Tengshe, and Lawrence White, as well as Drs. Wei-Tang Chang, Sharon Furtak, Matti Hämäläinen, and Norbert Kop o. This research was supported by the National Institutes of Health (NIH) grants R21DC010060, R01MH083744, R01HD040712, R01NS037462, R01NS048279, and K99EB015445. The research environment was supported by the NIH/National Institute of Biomedical Imaging and Bioengineering (NIBIB) grant P41EB015896 (Center for Functional Neuroimaging Techniques, CFNT), NIH Shared Instrumentation Grant S10-RR024694, and the Harvard Clinical and Translational Science Center (Harvard Catalyst; NCRR-NIH UL1 RR025758; NCRR-NIH UL1 TR000170). Author I.P.J. was supported by the Academy Of Finland grant 130412, and Author J.P.R. by the NIH grant R56NS052494 and by the National Science Foundation grant NSF PIRE-OISE-0730255.

References

1. Rauschecker JP, Tian B. Mechanisms and streams for processing of “what” and “where” in auditory cortex. *Proc Natl Acad Sci U S A*. 2000; 97:11800–11806. [PubMed: 11050212]
2. Tian B, Reser D, Durham A, Kustov A, Rauschecker JP. Functional specialization in rhesus monkey auditory cortex. *Science*. 2001; 292:290–293. [PubMed: 11303104]
3. Ahveninen J, et al. Task-modulated “what” and “where” pathways in human auditory cortex. *Proc Natl Acad Sci U S A*. 2006; 103:14608–14613. [PubMed: 16983092]
4. Lomber SG, Malhotra S. Double dissociation of ‘what’ and ‘where’ processing in auditory cortex. *Nat Neurosci*. 2008; 11:609–616. [PubMed: 18408717]
5. Romanski LM, et al. Dual streams of auditory afferents target multiple domains in the primate prefrontal cortex. *Nat Neurosci*. 1999; 2:1131–1136. [PubMed: 10570492]
6. Clarke S, Bellmann A, Meuli RA, Assal G, Steck AJ. Auditory agnosia and auditory spatial deficits following left hemispheric lesions: evidence for distinct processing pathways. *Neuropsychologia*. 2000; 38:797–807. [PubMed: 10689055]
7. Alain C, Arnott SR, Hevenor S, Graham S, Grady CL. “What” and “where” in the human auditory system. *Proc Natl Acad Sci U S A*. 2001; 98:12301–12306. [PubMed: 11572938]
8. Maeder PP, et al. Distinct pathways involved in sound recognition and localization: a human fMRI study. *Neuroimage*. 2001; 14:802–816. [PubMed: 11554799]
9. Bushara KO, et al. Modality-specific frontal and parietal areas for auditory and visual spatial localization in humans. *Nat Neurosci*. 1999; 2:759–766. [PubMed: 10412067]
10. Barrett DJ, Hall DA. Response preferences for “what” and “where” in human non-primary auditory cortex. *Neuroimage*. 2006; 32:968–977. [PubMed: 16733092]
11. Warren JD, Zielinski BA, Green GG, Rauschecker JP, Griffiths TD. Perception of sound-source motion by the human brain. *Neuron*. 2002; 34:139–148. [PubMed: 11931748]
12. Brunetti M, et al. Human brain activation during passive listening to sounds from different locations: an fMRI and MEG study. *Hum Brain Mapp*. 2005; 26:251–261. [PubMed: 15954141]
13. Deouell LY, Heller AS, Malach R, D’Esposito M, Knight RT. Cerebral responses to change in spatial location of unattended sounds. *Neuron*. 2007; 55:985–996. [PubMed: 17880900]
14. Kopco N, et al. Neuronal representations of distance in human auditory cortex. *Proc Natl Acad Sci U S A*. 2012; 109:11019–11024. [PubMed: 22699495]
15. Patterson RD, Uppenkamp S, Johnsrude IS, Griffiths TD. The processing of temporal pitch and melody information in auditory cortex. *Neuron*. 2002; 36:767–776. [PubMed: 12441063]
16. Puschmann S, Uppenkamp S, Kollmeier B, Thiel CM. Dichotic pitch activates pitch processing centre in Heschl’s gyrus. *Neuroimage*. 2010; 49:1641–1649. [PubMed: 19782757]

17. Binder JR, et al. Human temporal lobe activation by speech and nonspeech sounds. *Cereb Cortex*. 2000; 10:512–528. [PubMed: 10847601]
18. Scott SK, Blank CC, Rosen S, Wise RJ. Identification of a pathway for intelligible speech in the left temporal lobe. *Brain*. 2000; 123:2400–2406. [PubMed: 11099443]
19. Obleser J, et al. Vowel sound extraction in anterior superior temporal cortex. *Hum Brain Mapp*. 2005
20. DeWitt I, Rauschecker JP. Phoneme and word recognition in the auditory ventral stream. *Proc Natl Acad Sci U S A*. 2012; 109:E505–514. [PubMed: 22308358]
21. Thivard L, Belin P, Zilbovicius M, Poline JB, Samson Y. A cortical region sensitive to auditory spectral motion. *NeuroReport*. 2000; 11:2969–2972. [PubMed: 11006976]
22. Griffiths TD, Warren JD. The planum temporale as a computational hub. *Trends in Neurosciences*. 2002; 25:348–353. [PubMed: 12079762]
23. Zatorre RJ, Evans AC, Meyer E, Gjedde A. Lateralization of phonetic and pitch discrimination in speech processing. *Science*. 1992; 256:846–849. [PubMed: 1589767]
24. Belin P, Zatorre RJ. ‘What’, ‘where’ and ‘how’ in auditory cortex. *Nature Neuroscience*. 2000; 3:965–966. [PubMed: 11017161]
25. Recanzone GH, Cohen YE. Serial and parallel processing in the primate auditory cortex revisited. *Behav Brain Res*. 2010; 206:1–7. [PubMed: 19686779]
26. Adriani M, et al. Sound recognition and localization in man: specialized cortical networks and effects of acute circumscribed lesions. *Exp Brain Res*. 2003; 153:591–604. [PubMed: 14504861]
27. Clarke S, et al. What and where in human audition: selective deficits following focal hemispheric lesions. *Exp Brain Res*. 2002; 147:8–15. [PubMed: 12373363]
28. Payne BR, Lomber SG. A method to assess the functional impact of cerebral connections on target populations of neurons. *J Neurosci Methods*. 1999; 86:195–208. [PubMed: 10065986]
29. Vanduffel W, Payne BR, Lomber SG, Orban GA. Functional impact of cerebral connections. *Proc Natl Acad Sci U S A*. 1997; 94:7617–7620. [PubMed: 9207141]
30. Clarey JC, Tweedale R, Calford MB. Interhemispheric modulation of somatosensory receptive fields: evidence for plasticity in primary somatosensory cortex. *Cereb Cortex*. 1996; 6:196–206. [PubMed: 8670650]
31. Wilke M, Kagan I, Andersen RA. Functional imaging reveals rapid reorganization of cortical activity after parietal inactivation in monkeys. *Proc Natl Acad Sci U S A*. 2012; 109:8274–8279. [PubMed: 22562793]
32. Calford MB, Tweedale R. Interhemispheric transfer of plasticity in the cerebral cortex. *Science*. 1990; 249:805–807. [PubMed: 2389146]
33. Werhahn KJ, Mortensen J, Kaelin-Lang A, Boroojerdi B, Cohen LG. Cortical excitability changes induced by deafferentation of the contralateral hemisphere. *Brain*. 2002; 125:1402–1413. [PubMed: 12023328]
34. Popelar J, Nwabueze-Ogbo FC, Syka J. Changes in neuronal activity of the inferior colliculus in rat after temporal inactivation of the auditory cortex. *Physiol Res*. 2003; 52:615–628. [PubMed: 14535838]
35. Kujirai T, et al. Corticocortical inhibition in human motor cortex. *J Physiol*. 1993; 471:501–519. [PubMed: 8120818]
36. Oliveri M, et al. Paired transcranial magnetic stimulation protocols reveal a pattern of inhibition and facilitation in the human parietal cortex. *J Physiol*. 2000; 529(Pt 2):461–468. [PubMed: 11101654]
37. Ilic TV, et al. Short-interval paired-pulse inhibition and facilitation of human motor cortex: the dimension of stimulus intensity. *J Physiol*. 2002; 545:153–167. [PubMed: 12433957]
38. Gough PM, Nobre AC, Devlin JT. Dissociating linguistic processes in the left inferior frontal cortex with transcranial magnetic stimulation. *J Neurosci*. 2005; 25:8010–8016. [PubMed: 16135758]
39. Collignon O, et al. Time-course of Posterior Parietal and Occipital Cortex Contribution to Sound Localization. *J Cogn Neurosci*. 2008

40. At A, Spierer L, Clarke S. The role of the right parietal cortex in sound localization: a chronometric single pulse transcranial magnetic stimulation study. *Neuropsychologia*. 2011; 49:2794–2797. [PubMed: 21679720]
41. Lewald J, Staedtgen M, Sparing R, Meister IG. Processing of auditory motion in inferior parietal lobule: evidence from transcranial magnetic stimulation. *Neuropsychologia*. 2011; 49:209–215. [PubMed: 21130790]
42. Baayen RH, Davidson DJ, Bates DM. Mixed-effects modeling with crossed random effects for subjects and items. *Journal of Memory and Language*. 2008; 59:390–412.
43. Baayen RH, Milin P. Analyzing reaction times. *Int J Psychol Res*. 2010:12–28.
44. Pascual-Leone A, Walsh V, Rothwell J. Transcranial magnetic stimulation in cognitive neuroscience--virtual lesion, chronometry, and functional connectivity. *Curr Opin Neurobiol*. 2000; 10:232–237. [PubMed: 10753803]
45. Lu ZL, Williamson SJ, Kaufman L. Behavioral lifetime of human auditory sensory memory predicted by physiological measures. *Science*. 1992; 258:1668–1670. [PubMed: 1455246]
46. Jääskeläinen IP, et al. Human posterior auditory cortex gates novel sounds to consciousness. *Proc Natl Acad Sci U S A*. 2004; 101:6809–6814. [PubMed: 15096618]
47. Stecker GC, Mickey BJ, Macpherson EA, Middlebrooks JC. Spatial sensitivity in field PAF of cat auditory cortex. *J Neurophysiol*. 2003; 89:2889–2903. [PubMed: 12611946]
48. Salminen NH, May PJ, Alku P, Tiitinen H. A population rate code of auditory space in the human cortex. *PLoS One*. 2009; 4:e7600. [PubMed: 19855836]
49. Hall DA, Plack CJ. Pitch processing sites in the human auditory brain. *Cereb Cortex*. 2009; 19:576–585. [PubMed: 18603609]
50. Bendor D, Wang X. The neuronal representation of pitch in primate auditory cortex. *Nature*. 2005; 436:1161–1165. [PubMed: 16121182]
51. Griffiths TD, Buchel C, Frackowiak RS, Patterson RD. Analysis of temporal structure in sound by the human brain. *Nat Neurosci*. 1998; 1:422–427. [PubMed: 10196534]
52. Rauschecker JP, Scott SK. Maps and streams in the auditory cortex: nonhuman primates illuminate human speech processing. *Nat Neurosci*. 2009; 12:718–724. [PubMed: 19471271]
53. Rossi S, Hallett M, Rossini PM, Pascual-Leone A. Safety of, T.M.S.C.G. Safety, ethical considerations, and application guidelines for the use of transcranial magnetic stimulation in clinical practice and research. *Clin Neurophysiol*. 2009; 120:2008–2039. [PubMed: 19833552]
54. Algazi, VR.; Duda, RO.; Thompson, M.; Avendano, C. IEEE Workshop on Applications of Signal Processing to Audio and Electroacoustics. Mohonk Mountain House; New Paltz, NY: 2001. The CIPIC HRTF database; p. 99-102.
55. Nummenmaa A, et al. Comparison of spherical and realistically shaped boundary element head models for transcranial magnetic stimulation navigation. *Clin Neurophysiol*. 2013
56. Stenroos M, Mantynen V, Nenonen J. A Matlab library for solving quasi-static volume conduction problems using the boundary element method. *Comput Methods Programs Biomed*. 2007; 88:256–263. [PubMed: 18022274]
57. Fischl B, Sereno M, Dale A. Cortical surface-based analysis. II: Inflation, flattening, and a surface-based coordinate system. *Neuroimage*. 1999; 9:195–207. [PubMed: 9931269]
58. Bates DM, Maechler M. lme4: Linear mixed-effects models using S4 classes. R package version 0.999999-0. 2009
59. Team, R.D.C. R: a language and environment for statistical computing. R Foundation for Statistical Computing; Vienna: 2009.
60. Lenth RV. lsmeans: least-squares means. R Package version 1.06-05. 2013

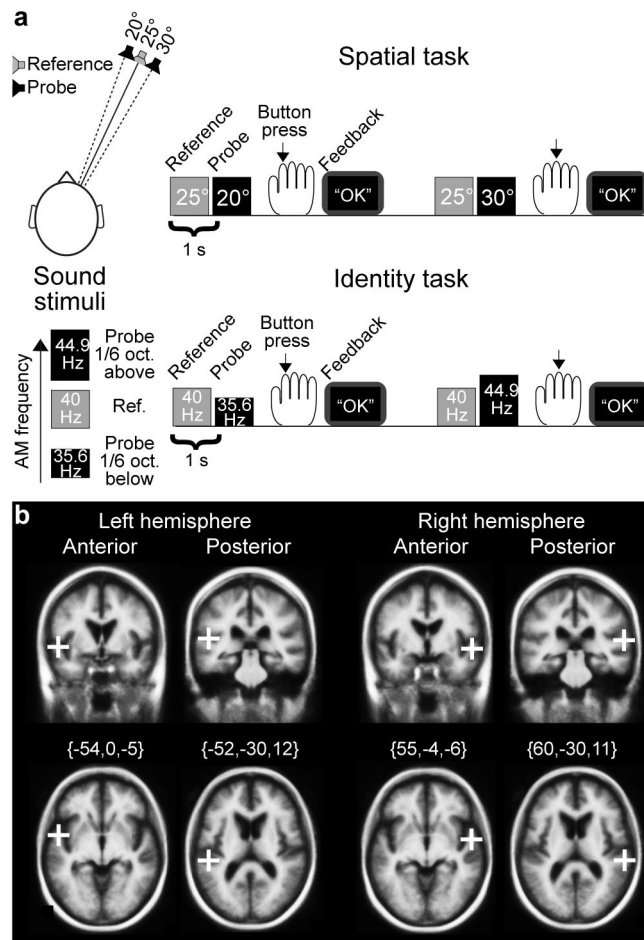


Figure 1.

Study design. **(a)** Stimuli and tasks. In the Spatial task, subjects discriminated whether Probe was simulated from 5° to the left or 5° to the right relative to Reference (25° to the right). In the Identity task, subjects discriminated whether Probe sound had $1/6$ octaves lower or higher AM frequency than the AM frequency of Reference (40 Hz). Feedback was presented at a computer screen after each trial in both tasks. **(b)** Initial TMS target locations. In 50% of the trials, paired TMS pulses were delivered 55–145 ms after Probe sound onsets, bilaterally to either the posterior or anterior target regions of AC, shown here in the Freesurfer standard brain (i.e., Montreal Neurological Institute 305; MNI305) in Talairach coordinates. For each subject, target regions were transformed through the Talairach coordinate systems. Using navigated TMS, the coil was positioned to maximally stimulate the cortical area of interest. After the experiments, TMS-induced E-fields were estimated in each subject's cortical surface using physical modeling, to localize the maximally stimulated AC subregions (Fig 4).

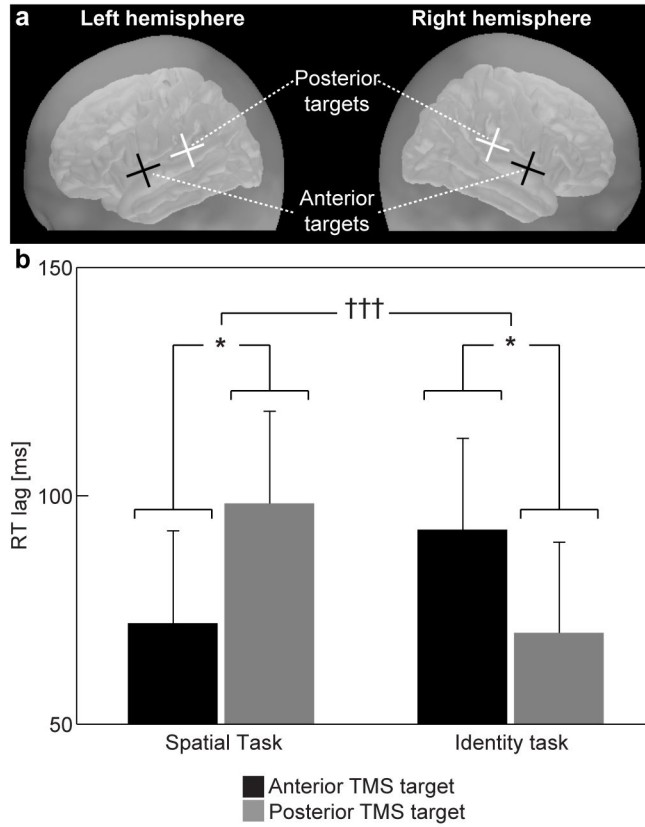


Figure 2. TMS-induced RT lags during Spatial and Identity tasks. **(a)** Schematic illustration of the approximate TMS coil center locations during bilateral anterior *vs.* posterior stimulation. **(b)** Estimated marginal means and standard errors of RT lags derived from the linear mixed model, with the different stimulation latencies pooled together ($N=10$). These data show a significant interaction between the task and TMS target factors, suggesting brain location-specific performance modulations during auditory Identity *vs.* Spatial tasks. This result provides causal support for the theory of two distinct AC areas for sound identity and location processing^{1, 2}, which has previously been suggested in humans based on neuroimaging activation studies. ††† $P_{MCMC} = 0.001$, task by target location interaction of the linear mixed model; * $P < 0.05$, *a priori* comparison of task-specific effects across the TMS target loci derived from the linear mixed model.

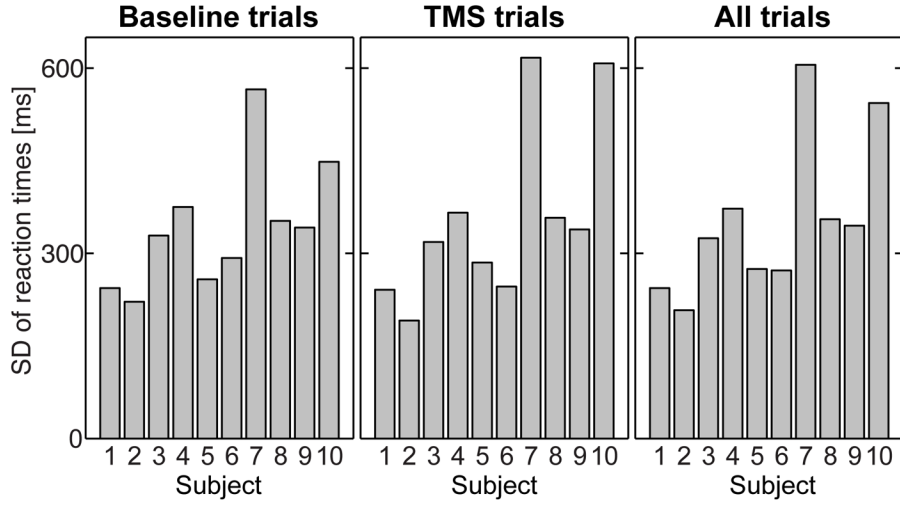


Figure 3. Standard deviation of individual-trial RTs in the population of 10 subjects. SDs of RTs are shown during trials without TMS (left), during TMS (middle), and across all trials (right). The variance of RT performance was relatively homogeneous across subjects, apart from two subjects (7 and 10) that demonstrated a higher level of variance than the other subjects. This potential bias was taken into account in the linear mixed model by using least-squares weighting of the regression coefficients by the inverse variance of each subjects' behavioral performance.

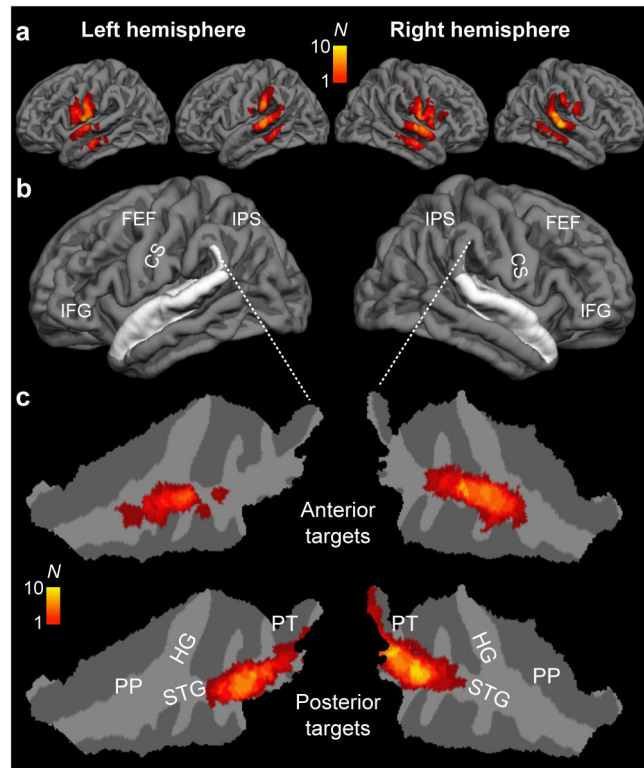


Figure 4.

Modeling of TMS-induced E-fields in the cortex. **(a)** Distribution of TMS effects exceeding 80% motor threshold (MT) strength during TMS in all subjects ($N=10$), shown on a standard brain cortical reconstruction. **(b)** Gross anatomical landmarks of interest shown on the standard-brain cortex. The location of superior temporal cortices, which encompass ACs has been shown in white. The loci of central sulcus (CS), and extra-AC areas related to “what” (inferior frontal gyrus, IFG) and “where” (intraparietal sulcus, IPS; frontal eye fields, FEF) processing streams are also shown. **(c)** TMS-induced electric fields in AC on flattened patches of the superior temporal cortices. Taken together, our modeling results demonstrate that TMS-induced E-fields were successfully delivered at the posterior (posterior STG, PT) vs. anterior AC areas (anterior STG, PP), hypothesized to be associated with sound location vs. identity feature discrimination, respectively. As expected, TMS also induced E-fields in the adjacent cortical gyri. However, the panel **a** shows that these fields were not close to the frontoparietal areas typically associated with extra-AC “where” (IPS/FEF) and “what” (IFG) processing. The color scale depicts the number of subjects with stimulation reaching the threshold at a given location.

Table 1

Group-average RTs in milliseconds.

	Baseline	TMS pulse-pair latency			
		55 ms	85 ms	115 ms	145 ms
Spatial task	Anterior AC	729 ± 128	803 ± 160	796 ± 189	768 ± 113
	Posterior AC	682 ± 107	755 ± 173	772 ± 125	749 ± 136
Identity task	Anterior AC	719 ± 147	827 ± 200	779 ± 221	790 ± 224
	Posterior AC	707 ± 85	781 ± 115	746 ± 96	734 ± 128

Inverse-variance weighted group mean ± standard deviation is shown for each task condition, TMS target location, and stimulation latency (N=10).

Table 2

Group-average HR percentages.

	Baseline	TMS pulse-pair latency				
		55 ms	85 ms	115 ms	145 ms	
Spatial task	Anterior AC	85 ± 14	66 ± 15	69 ± 17	68 ± 11	78 ± 13
	Posterior AC	85 ± 8	69 ± 14	70 ± 23	69 ± 17	75 ± 22
Identity task	Anterior AC	91 ± 12	87 ± 19	87 ± 16	91 ± 17	89 ± 12
	Posterior AC	90 ± 11	86 ± 19	89 ± 20	87 ± 18	86 ± 16

Inverse-variance weighted group mean ± standard deviation is shown for each task condition, TMS target location, and pulse latency (N=10).